Heterozygous germline mutations in A2ML1 are associated with a disorder clinically related to Noonan syndrome

Lisenka E.L.M.Vissers[1,2,3,11,] Monica Bonetti[4,11], Jeroen Paardekooper Overman[4,11], Willy M. Nillesen[1], Suzanna G.M. Frints[5], Joep de Ligt[1,2,3], Giuseppe Zampino[6], Ana Justino[7], José C.Machado[7], Marga Schepens[1], Han G. Brunner[1,2,3], Joris A. Veltman[1,2,3], Hans Scheffer[1], Piet Gros[8], José L. Costa[7], Marco Tartaglia[9], Ineke van der Burgt[1,12], Helger G Yntema[1,2,12,*], and Jeroen den Hertog[4,10,12]

1Department of Human Genetics, Radboud university medical center, Nijmegen, The Netherlands; 2Radboud Institute for Molecular Life Sciences, Radboud university medical center, Nijmegen, The Netherlands; 3Donders Centre for Neuroscience, Radboud university medical center, Nijmegen, The Netherlands; 4Hubrecht Institute-KNAW and University Medical Center, Utrecht, The Netherlands; 5Department of Clinical Genetics, Maastricht University Medical Centre, Maastricht, The Netherlands; 6Dipartimento di Pediatria, Università Cattolica del Sacro Cuore, Rome, Italy; 7IPATIMUP - Institute of Molecular Pathology and Immunology of the University of Porto, Porto, Portugal; 8Crystal and Structural Chemistry, Bijvoet Center for Biomolecular Research, Department of Chemistry, Faculty of Science, Utrecht University, Utrecht, the Netherlands; 9Dipartimento di Ematologia, Oncologia e Medicina Molecolare, Istituto Superiore di Sanità, Rome, Italy; 10Institute of Biology, Leiden, The Netherlands; 11These authors contributed equally to this work; 12These authors jointly directed this work

European Journal of Human Genetics, 2014 Jun 18

Abstract

Noonan syndrome (NS) is a developmental disorder characterized by short stature, facial dysmorphisms and congenital heart defects. To date, all mutations known to cause NS are dominant, activating mutations in signal transducers of the RAS/MAPK pathway. In 25% of cases, however, the genetic cause of NS remains elusive, suggesting that factors other than those involved in the canonical RAS/MAPK pathway may also play a role. Here, we used family-based whole exome sequencing of a case-parent trio and identified a *de novo* mutation, p.(Arg802His), in *A2ML1* which encodes the secreted protease inhibitor Alpha-2-Macroglobulin-Like-1. Subsequent resequencing of *A2ML1* in 155 cases with a clinical diagnosis of NS led to the identification of additional mutations in two families, p.(Arg802Leu) and p.(Arg592Leu). Functional characterization of these human *A2ML1* mutations in zebrafish showed NS-like developmental defects, including a broad head, blunted face and cardiac malformations. Using the crystal structure of A2M, which is highly homologous to A2ML1, we identified the intramolecular interaction partner of p.Arg802. Mutation of this residue, p.Glu906, induced similar developmental defects in zebrafish, strengthening our conclusion that mutations in *A2ML1* cause a disorder clinically related to NS. This is the first report of the involvement of an extracellular factor in a disorder clinically related to RASopathies, providing potential new leads for better understanding of the molecular basis of this family of developmental diseases.

Introduction

Noonan syndrome (NS) is an autosomal dominant, clinically variable condition, with an estimated prevalence of 1 in 1,000-2,500.[1] NS patients are characterized by facial dysmorphism, a wide spectrum of cardiac disease, reduced postnatal growth, variable cognitive deficits, ectodermal and skeletal defects.[2-4] Congenital heart defects are observed in a large proportion of NS patients, in particular pulmonary stenosis (66%), and hypertrophic cardiomyopathy (14%).[5] Other relatively frequent clinical features of NS patients include webbed neck, cryptorchidism, bleeding tendency, and hydrops fetalis. NS is genetically heterogeneous and mutations in *PTPN11, SOS1*, *KRAS*, *NRAS*, *RAF1*, *BRAF*, *SHOC2*, *CBL* and *RIT1* account for approximately 75% of affected individuals.[4,6] To date, all mutations causing NS result in enhanced activation of signal transducers belonging to the RAS-mitogen activated protein kinase (MAPK) pathway.[7]

To identify new genetic causes of NS, we used a family-based whole-exome-sequencing approach in a patient-parent trio with sporadic disease to detect *de novo* changes in the proband. Genetic testing had previously excluded mutations in known NS genes. We identified a *de novo* mutation in *A2ML1*, which encodes the secreted protease inhibitor Alpha-2-Macroglobulin-Like-1 (A2ML1). *A2ML1* was re-sequenced in a cohort of cases with a clinical diagnosis of NS. Moreover, to provide more evidence for the involvement of the gene in this disorder resembling NS, protein modeling was performed and A2ML1 mutants were functionally characterized in zebrafish.

Results

Exome sequencing in a NS case-parent trio

Exome sequencing in case 1 (Figure 1A) and her parents revealed four potential *de novo* mutations, two of which were validated by Sanger sequencing and confirmed to be of *de novo* origin (Supplementary Table 1). The first mutation is predicted to lead to p.(Arg129Pro) in *OR12D3* (NM_030959.2:c.386G>C), encoding an olfactory receptor. Based on the function of the gene product (odor perception) combined with the low evolutionary conservation at base pair level (PhyloP 0.55), we do not consider this variant to be relevant for the phenotype of the patient, but assume that this *de novo* mutation reflects the human per-generation background mutation rate. [16] The second *de novo* mutation was detected in *A2ML1* (NM_144670.3:c.2405G>A) and is predicted to lead to p.(Arg802His). This *de novo* mutation occurred at a highly conserved nucleotide (PhyloP 3.41) and affects a residue within the alpha-2-macroglobulin domain (Figure 2A). It is noteworthy that the c.2405G>A variant in *A2ML1* is also reported in 4/12,194 alleles in the NHLBI Exome Sequencing Project (ESP) (http://evs.gs.washington.edu/EVS/). Further analysis of the ESP database indicated that several frequently reported causal mutations in known NS genes, including *PTPN11*, are described in this database at similar frequency (Table 2).

Mutation analysis of the A2ML1 gene in a NS cohort

Next, 155 individuals with a clinical diagnosis of NS were analyzed for mutations in *A2ML1* by direct Sanger sequencing and Ion PGM system. This screen led to the identification of two additional likely causal missense mutations in two unrelated individuals (Figure 1B-C, Table 2). The mutation identified in case 2, c.2405G>T, affects the same residue as identified in family 1 but is predicted to result in a different substitution, p.(Arg802Leu). Segregation analysis showed that the mutation is transmitted to his son (case 3), who is also diagnosed with the same disorder resembling NS. His mother (case 4), who does not show typical features of NS, also carries the

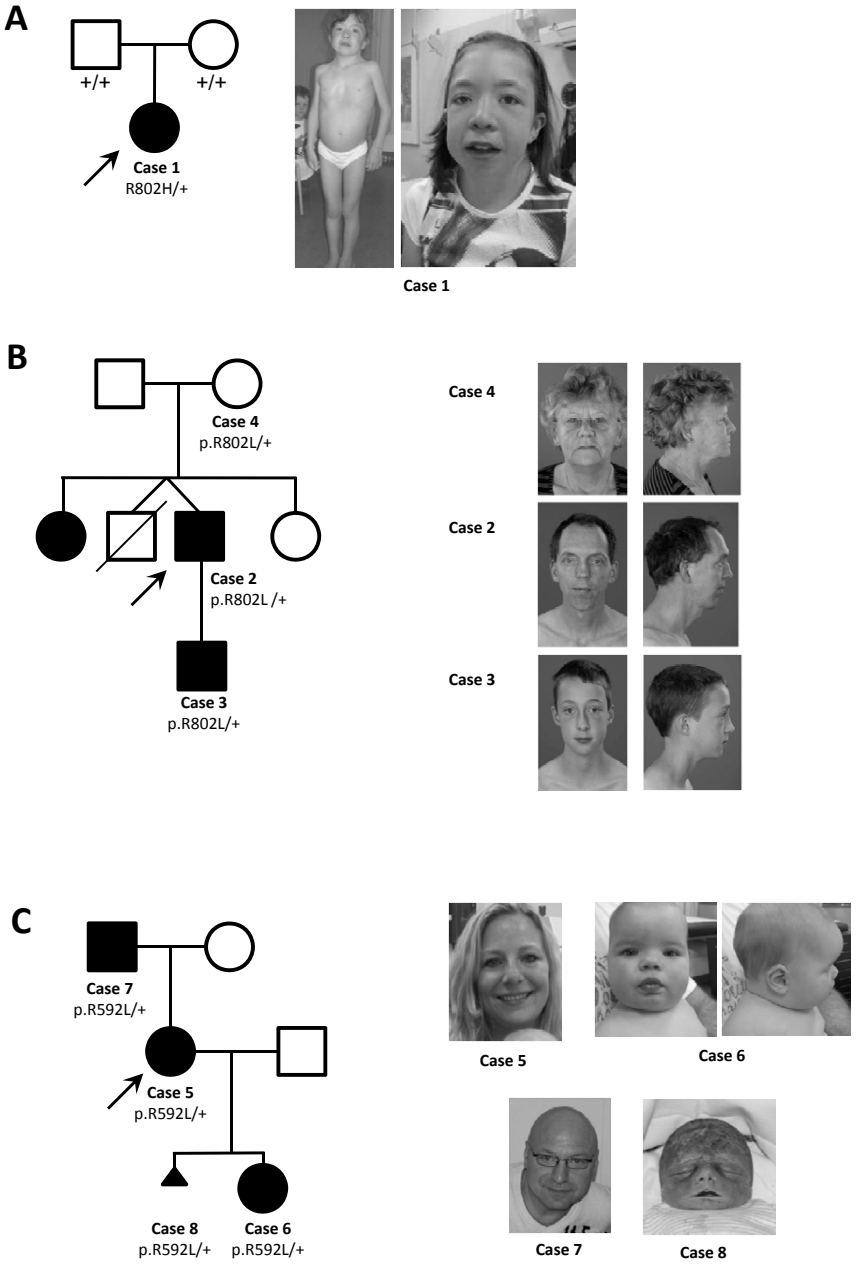

Figure 1. Photographs and pedigrees of families diagnosed with Noonan(-like) syndrome with likely pathogenic mutations in *A2ML1*. (A) Family 1 – case 1. *De novo* mutation p.(Arg802His); (B) Family 2 – cases 2, 3 and 4. Familial p.(Arg802Leu). The sister of case 2 is reported upon heteroanamnesis to have the same clinical phenotype. However, DNA nor detailed clinical information were available for this study. (C) Family 3 – cases 5, 6, 7 and 8. Familial p.(Arg592Leu). Clinical details of all cases are presented in Table 3. Note, the absence of genotypes for (un)affected family members indicates that DNA samples of these individuals were not available for testing. Black solid squares/circles represent clinically affected individuals, whereas as open squares/circles represent healthy individuals.

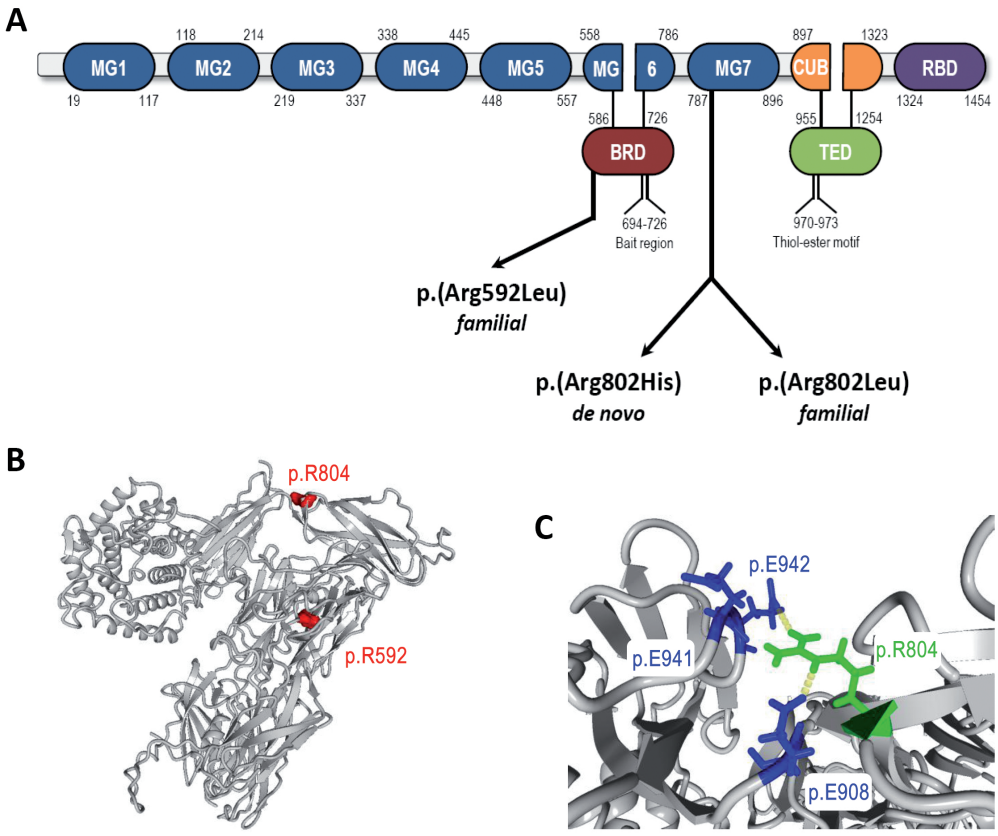

Figure 2. A2ML1 domain structure and modeling of the intramolecular interactions involving p.Arg802. (A) Schematic representation of A2ML1 protein domain structure and mutations in individuals with Noonan syndrome-like disorder. Numbers correspond to amino acid positions of A2ML1. MG: macroglobulin-like domain; BRD: bait region domain; CUB: complement C1r/C1s, Uegf, Bmp1 domain; TED: trioester domain; RBD: receptor binding domain. (B) Crystal structure of A2M (pdb code 4ACQ). Overall structure with p.Arg598 and p.Arg804 highlighted, corresponding to p.Arg592 and p.Arg802 in A2ML1, respectively. (C) Close-up of A2M-R804, corresponding to A2ML1-R802 (in green), which interacts with A2M-E908 (A2ML1-E906) (in blue) through hydrogen bonds (yellow dashed lines) and electrostatic interactions. A2M-E941 and A2M-E942 (in blue) may also interact with A2M-R802, but are not conserved in A2ML1 (p.P939 and p.D940, respectively).

mutation (Figure 1B). In the proband of family 3 (case 5), a c.1775G>T mutation (p.(Arg592Leu)) was detected. Familial segregation studies revealed the same mutation in her daughter (case 6) and her father (case 7), who were both clinically diagnosed with a disorder resembling NS (Figure 1C). Strikingly, the patient's first pregnancy resulted in intra-uterine fetal death at 29 weeks of gestation because of hydrops foetalis (case 8, Figure 1C). Pathological examination of the fetus showed facial features suggestive for NS. Molecular analysis of fetal DNA indicates maternal inheritance of the A2ML1 mutation p.(Arg592Leu). The clinical features of all individuals with an A2ML1 mutation are summarized in Table 3. A full description of the clinical data is provided in the supplement. Screening of selected exons of *A2ML1* in an additional cohort of 140 individuals with a clinical phenotype fitting or suggestive for NS did not reveal any pathogenic mutations. All variants detected are shown in Supplementary Table 2.

Protein modeling of mutations detected in A2ML1

All three *A2ML1* mutations, p.(Arg592Leu), p.(Arg802His) and p.(Arg802Leu), affect highly conserved residues among orthologs (Supplementary Figure 2). For protein modeling of the mutation locations and their predicted effect, the crystal structure of alpha-2-macroglobulin (A2M; pdb 4ACQ) was used (Figure 2, Table 1). A2ML1 is highly homologous to A2M and it is highly likely that protein folding of the two related proteins is similar (Supplementary Figure 1). Arginine 592, corresponding to A2M p.Arg598, is located at the edge of the Bait Region Domain and is buried in a large cavity on the back face of the A2ML1 monomer[17] whereas Arginine 802, corresponding to A2M p.Arg804, is located within macroglobulin-like domain 7 and is positioned more at the surface of the protein (Figure 2B). Mutations of either residue likely lead to conformational changes in A2ML1 by loss of hydrogen bonds or charge interactions. In more detail, within the intramolecular binding network, disease-associated mutations of p.Arg802 were predicted to disrupts the interaction with p.Glu906 (Figure 2C).

Functional consequences of A2ML1 mutations

A2ml1 is relative highly conserved in zebrafish (38% identity) and we investigated the functional consequences of expression of mutant A2ml1 on zebrafish development. *A2ml1* is predominantly expressed in the liver during embryonic development and morpholino-mediated knockdown of A2ml1 has previously been shown to induce defective liver development.[18] We introduced human A2ML1 mutations (p.R802H, p.R802L and p.S592L, human numbering for clarity, see Table 1) in zebrafish A2ml1, C-terminally fused with GFP, allowing to monitor (mutant) A2ml1 expression in tissue culture cells and during development (Supplementary Figure 3, 4).

Expression of most mutant NS-associated genes in tissue culture cells augments activation of the RAS/MAPK pathway, measurable by excessive ERK/MAPK phosphorylation in cycling cells. To investigate the effect of mutant A2ml1 on the RAS/MAPK pathway, we expressed mutant *A2ml1-gfp* fusion proteins in HEK-293T and COS7 cells to determine the levels of ERK/MAPK phosphorylation. Expression of *A2ml1* mutants in normally growing HEK-293T cells or in serum-stimulated COS7 cells did not significantly enhance ERK/MAPK phosphorylation (Supplementary Figure 3). These results suggest either that (mutant) A2ml1 does not modulate ERK/MAPK signaling, or that HEK-293T cells and COS7 cells are not responsive to (mutant) A2ml1. The effect of (mutant) A2ml1 on embryonic development was investigated by microinjection of CMV-promoter-driven expression vectors for wildtype or mutant A2ml1 in zebrafish embryos at the one-cell stage. Exogenous A2ml1-GFP was detected throughout the zebrafish embryo, despite mosaicism of the transgene, which is consistent with A2ml1-GFP being a secreted factor (Supplementary Figure 4).

Expression of mutant A2ml1 resulted in developmental defects in zebrafish embryos that involved the heart and craniofacial structures, whereas expression of GFP alone or wildtype A2ml1 did not affect zebrafish development (Figure 3). The morphological defects elicited by mutant A2ml1 resembled those induced by NS-associated Shp2-D61G and N-Ras-I24N.[12,19] Of note, A2ml1-mutation-induced morphological defects appeared later in development (apparent from 3dpf onwards) and were less severe than those observed for Shp2-D61G-induced defects (from 6hpf onwards). Alcian blue staining of cartilaginous structures in 4dpf zebrafish embryos revealed craniofacial defects that are characteristic of NS. Morphometric analysis showed statistically significant broadening of the head and blunting of the faces in embryos expressing mutant A2ml1 (Figure 3B). Also, *in situ* hybridization using the heart-specific probe *myl7* (formerly known as

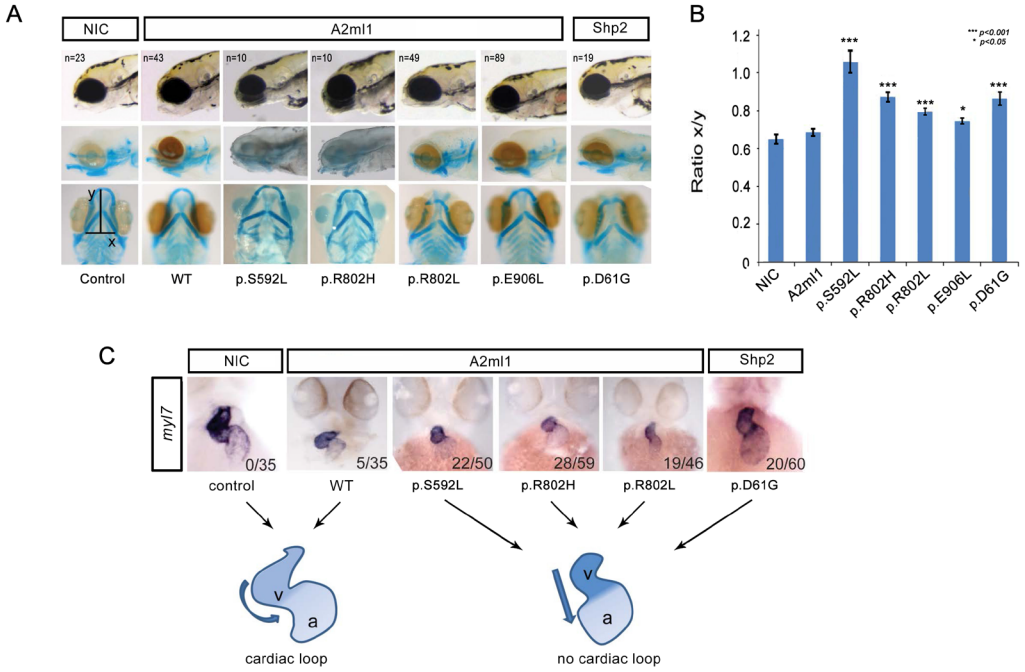

Figure 3. Mutant A2ml1 causes a developmental disorder resembling NS. (A) Expression of mutant A2ml1 results in developmental defects in zebrafish embryos at 4dpf. The craniofacial defects were highlighted by cartilage staining using alcian blue. The heads are broader and the faces blunted. 'n' refers to the number of embryos examined for x/y ratio. (B) To quantify the craniofacial defects, the ratio of the width of the ceratohyal and the distance to Meckel's cartilage (x and y, respectively in bottom left panel of A) was determined. The averages are plotted, error bars indicate standard error of the mean. Student t-test to compare ratios with non-injected control (NIC) indicate that wild type A2ml1 is not significantly different, but mutant A2ml1 and mutant Shp2 are significantly enhanced compared to NIC as indicated. Note that human numbering of residues was used for A2ml1 mutants. (C) *In situ* hybridization of 55hpf embryos using a heart-specific probe (*myl7*) which stains cardiomyocytes. Cardiac looping was assessed as normal looping (loop) or impaired looping (no loop) as indicated schematically. The number of no loop hearts in embryos expressing mutant A2ml1 or mutant Shp2 / total number of embryos is indicated in the bottom right corner of each panel.

cmlc2) indicated that cardiac looping was impaired in mutant *a2ml1*-injected embryos in a similar manner as in Shp2-D61G expressing embryos (Figure 3C). Protein modeling suggested that the p.(Arg802His) and p.(Arg802Leu) mutations would lead to a loss of the interaction between p. Arg802 and p.Glu906. Therefore, p.Glu906 was mutated to leucine and this mutant was expressed in zebrafish embryos to study the functional defect. Expression of mutant A2ml1-E906L induced developmental defects to a similar extent as NS-associated A2ml1-R802L mutants (Figure 3B), further supporting a causal role of A2ml1 mutations involving substitution of p.Arg802.

Discussion

Analysis of a case-parent trio with a clinical suspicion of NS revealed a *de novo* mutation in *A2ML1* (c.2405G>A; p.(Arg802His)). A2ML1 encodes the protease inhibitor A2ML1, which is a member of the alpha-macroglobulin superfamily of proteins that contains both complement components and protease inhibitors. These proteins display a unique trap mechanism of inhibition, by which the alpha-2-macroglobulin inhibitor undergoes a major conformational change upon its cleavage by a protease, thereby trapping the protease and blocking it from subsequent substrate binding.[20]

Moreover, A2ML1 binds to the lipoprotein receptor-related protein 1 (LRP1) receptor[21], an upstream activator of the MAPK/Extracellular signal-regulated kinase (ERK) cascade.[22] Additionally, LRP1 directly interacts with CBL.[23] Together, these reports suggest that A2ML1 may act upstream of signaling pathways known to be involved in NS.

Two additional missense mutations in families with a disorder clinically resembling NS were identified by Sanger sequencing of the entire coding region of the gene (c.2405G>T; p.(Arg802Leu), and c.1775G>T; (p.(Arg592Leu)). The frequency of *A2ML1* mutations in the cohort tested in this study is therefore approximately 1%. However, since mutations in the major NS genes had already been excluded, the contribution of A2ML1 mutations to the total population clinically diagnosed with NS is expected to be less than 0.5%. The fact that two of the three A2ML1 mutations have been reported in the EVS database with a frequency comparable to that in the NS patients, could either mean that the A2ML1 mutations are not pathogenic, or that the phenotypic features of people with an *A2ML1* mutation is milder and they are unrecognized in the general population (making *A2ML1* a relatively high frequency gene in mild NS). The fact that case 4 does not show phenotypic features of NS would fit both of these theories, since cases with non-penetrance, which albeit very rare, have previously been described in NS.[24] Evidence for the pathogenicity of the *A2ML1* mutations therefore had to be provided by functional studies.
Whereas most NS-associated mutations have an effect on RAS/MAPK signaling, we did not detect RAS/MAPK activation in response to expression of *A2ml1* mutations in HEK293T cells or COS7 cells. Cell type specific MAPK activation by NS-associated genes is not unprecedented; NS-associated mutant SHOC2 enhances stimulus-induced MAPK activation in Neuro2A cells, but not in Cos-1 or 293T cells.[25] Hence, our results do not exclude involvement of A2ML1 in NS, but either suggest that A2ML1 does not modulate ERK/MAPK signaling, or that COS7 and HEK-293T cells are irresponsive to A2ML1. Future studies of A2ML1 variants in cell systems expressing LRP1 receptor might shed more light on the role of A2ML1 in ERK/MAPK signaling.

Expression of mutant A2ml1 in zebrafish embryos resulted in developmental defects that were characterized by craniofacial and cardiac defects, resembling those induced by expression of mutant Shp2. The A2ml1-mutation-induced morphological defects appear however later in development (apparent from 3dpf onwards) and are less severe than those observed for Shp2-D61G-induced defects (from 6hpf onwards). In line with this notion, the affected individuals in families 2 and 3, who transmitted the *A2ML1* mutation to their offspring, do not fulfill all classical van der Burgt criteria for NS[3], but present with a less severe phenotype suggestive of the disorder. Of note, phenotypic variability is well known for NS, and more explicitly, not all patients with NS have a cardiac malformation.[5,26] Also, the affected individuals in the two families with an *A2ML1* mutation do not have a heart defect, while the same mutations in zebrafish cause cardiac malformation. Zebrafish mutants of the most recently described NS gene, RIT1, show incomplete looping of the heart and hypoplastic heart chambers, while the heart phenotype was variable or even absent in patients with *RIT1* mutations.[6]

Finally, we hypothesized that a conformational change in A2ML1 is the underlying mechanism leading to the developmental defects resembling NS. This conformational change may lead to destabilization of A2ML1, or it may interfere with its trap mechanism of inhibition. Since both intragenic deletions of *A2ML1* (reported in the Database of Genomic Variants[27]), as well as frameshift mutations are detected in healthy controls (Supplementary Table 2), haploinsufficiency is highly unlikely as a the underlying disease mechanism. Given that the A2M family of proteins acts in multimeric complexes, it is expected that conformational changes might have a dominant

negative effect or lead to gain of function of the complex. Since mutation of p.Arg802 likely disrupts the interaction with p.Glu906, we reasoned that mutation of p.Glu906 should have the same effect on A2ML1 function as mutation of p.Arg802. Indeed, expression of mutant A2ml1-E906L induced developmental defects to a similar extent as NS-associated A2ml1-R802L mutants, providing additional support that A2ML1 is involved in NS.

In summary, our results provide evidence that mutations in *A2ML1* are a cause of Noonan-like syndrome, with a variable phenotype ranging from severe (resulting in intra-uterine fetal death) to very mild (or even non-penetrance). Although mutations in this gene did not lead to detectable enhanced activation of the RAS/MAPK pathway in HEK293T cells or COS7 cells, expression of A2ml1 mutants in zebrafish embryos induced developmental defects that are comparable to mutations of other NS genes. Thus, we identified a causal role of an extracellular factor in NS for the first time and our results pave the way for further exploration of the function of A2ML1, its binding partners/receptors, and other relevant extracellular cascades in the pathogenicity of NS.

Materials and Methods

Patients

The individual (case 1) selected for exome sequencing had a clinical diagnosis of NS based on the criteria defined by Van der Burgt *et al*. (2007)[3]. For Sanger sequencing of the *A2ML1* gene we obtained a total of 295 DNA samples from unrelated individuals with NS or a clinically related phenotype. All patients, including patient 1, had been tested negative for mutations in previously identified disease genes (*PTPN11*, *KRAS*, *SOS1*, *NRAS*, *SHOC2*, *CBL*, *RAF1*, *BRAF*, *MAP2K1*, *MAP2K2*, *HRAS*, and *RIT1*). These samples were collected from three genetic centers (35 patients selected by IPATIMUP, Porto, Portugal, 120 patients from the Department of Human Genetics, RUNMC, Nijmegen, the Netherlands and 140 patients from the Department of Pediatrics, Università Cattolica del Sacro Cuore (UCSC), and Department of Hematology, Oncology and Molecular Medicine, Istituto Superiore di Sanità (ISS), Rome, Italy). The clinical diagnosis for NS or suggestive of a related trait was made on the basis of standardized clinical criteria assessed by experienced clinical geneticists.

Genomic DNA from whole blood was extracted using standard protocols. This study was approved by the Review Boards of all participating institutions. Informed consent to participate in the study was obtained for all individuals as well as permission to publish photographs of individuals shown in Figure 1.

Exome sequencing for de novo variants

Exome sequencing was performed as described before.[8] In brief, exome enrichment was performed using a SOLiD optimized SureSelect Human Exome Kit (v1, 37Mb; Agilent), subsequently followed by SOLiDv3 PLUS sequencing. Read mapping and variant calling for the patient-parent trio was performed as described before.[8] All candidate *de novo* mutations present in the individual with NS were independently validated using Sanger sequencing.

Mutation analysis

For 120 individuals with NS from the department of Human Genetics, Nijmegen, the Netherlands and 35 individuals with NS from IPATIMUP, Porto, Portugal, all coding exons and flanking intronic sequences of A2ML1 were PCR amplified and analyzed by Sanger sequencing or the Ion PGM

system, respectively, using standardized protocols. All variants and protein codons are referred to according to NM_144670.3 using HGVS nomenclature. Mutations identified were checked for *de novo* occurrence whenever parental DNAs were available. For the 140 individuals with NS or a clinically related phenotype selected from the ISS and UCSC, Rome, Italy, exons 15, 16, 19, 24, 25, 26, 29, 31 and 32 and flanking intronic sequences were considered, based on the identification of possible pathogenic mutations in the first cohort. For all variants detected, an *in-silico*-based method was used to assess the effect of the mutation (Alamut software, version 2.1; http://www.interactive-biosoftware.com/) in addition to an assessment of variant pathogenicity according to guidelines by the CMGS and VKGL, for the British and Dutch Molecular Genetic Societies respectively.[9]

Protein modeling of mutations identified in A2ML1

Pathogenic mutations were modeled for their effect on protein function. Because the three-dimensional structure of A2ML1 (Uniprot entry A8K2U0) is unknown, protein modeling was performed using PDB entry 4ACQ which represents the crystal structure of A2M. Overall, A2M and A2ML1 share 40% sequence identity. Mutations used for modeling occur within a sequence stretch that is highly conserved (Supplementary Figure 1). Graphical representations for mutations modeled on 4ACQ were generated and analyzed through project HOPE and YASARA.[10,11] Residue numbers in the paper are based on residues in A2ML1 (not 4ACQ). The residues in A2ML1 and their counterparts in 4ACQ and zebrafish (see section below) are listed in Table 1.

Cell culture, transfection and immunoblotting

COS7 cells and 293T cells were maintained using standard protocols and transfected using polyethyleneimine (PEI) (Sigma). Cells were lysed directly in 2x SDS sample buffer (125mM Tris-HCl pH 6.8, 20% glycerol, 4% SDS, 2% β-mercatoethanol and 0.04% bromophenol blue) and boiled. Lysates were separated on a 10% SDS-polyacrylamide gel and blotted using mouse anti-pERK, rabbit anti-ERK (Cell Signalling Technologies) and rabbit anti-GFP (Torrey Pines Biolabs). Enhanced chemiluminescence was used to detect signal from HRP conjugated secondary antibodies (BD Bioscience).

Zebrafish injections and in situ hybridization

Zebrafish were kept and embryos were raised under standard conditions. Zebrafish *a2ml1* (GenBank: BC125959.1) was cloned into pCS2+. Mutants were derived by PCR and verified by sequencing. The gene encoding *eGFP* was fused in frame to the 3'end of (mutant) *a2ml1* which allows monitoring of expression of (mutant) A2ml1 protein in zebrafish embryos. Cytomegalovirus (CMV)-driven expression vectors for (mutant) A2ml1, *CMV:a2ml1-egfp*, were injected into zebrafish embryos at the one-cell stage. Synthetic RNA encoding mutant Shp2-D61G was injected at the one cell stage as a control.[12] Morphological phenotypes were assessed at 4 days post fertilization (dpf). Embryos were anesthesized at 4 dpf with MS-222 (Sigma), fixed in 4% PFA and the cartilage was stained with alcian blue. The width of the ceratohyal and the distance to the tip of Meckel's cartilage were determined using Image J software[13] and the ratio was determined as a direct measure for craniofacial defects. Averages were determined and a student t-test was done to determine whether the differences between the different conditions were statistically significant. To investigate cardiac defects, embryos were fixed at 55 hpf and *in situ* hybridizations were done essentially as described[14] using probes specific for *myl7*.[15]

Deposition of genetic data

The data obtained in this study are submitted to LOVD, an online gene-centered collection and display of DNA variations (http://databases.lovd.nl/shared/genes).

Acknowledgements

We thank Hanka Venselaar for bioinformatics support in protein modeling and Martina Ruiterkamp-Versteeg, Petra de Vries, Suzanne Keijzers-Vloet, and Martine van Zweeden for technical assistance. This work was funded, in part, by a grant from the Research Council for Earth and Life Sciences (ALW 819.02.021) with financial aid from the Netherlands Organisation for Scientific Research (NWO) (to J.d.H.), Telethon-Italy (GGP13107; to M.T.), Fundação para a Ciência e Tecnologia (PTDC/BIM-MEC/0650/2012; to JLC), and PPS5 Consórcio DoIT (ADI–Agência de Inovação; to JLC). IPATIMUP is an Associate Laboratory of the Portuguese Ministry of Education and Science and is partially supported by FCT, the Portuguese Foundation for Science and Technology.

References

1. Mendez HM, Opitz JM (1985) Noonan syndrome: a review. Am J Med Genet 21: 493-506.
2. Allanson JE (1987) Noonan syndrome. J Med Genet 24: 9-13.
3. van der Burgt I (2007) Noonan syndrome. Orphanet J Rare Dis 2: 4.
4. Roberts AE, Allanson JE, Tartaglia M, Gelb BD (2013) Noonan syndrome. Lancet 381: 333-342.
5. Colquitt JL, Noonan JA (2013) Cardiac Findings in Noonan Syndrome on Long-term Follow-up. Congenit Heart Dis.
6. Aoki Y, Niihori T, Banjo T, Okamoto N, Mizuno S, et al. (2013) Gain-of-Function Mutations in RIT1 Cause Noonan Syndrome, a RAS/MAPK Pathway Syndrome. Am J Hum Genet 93: 173-180.
7. Tartaglia M, Gelb BD, Zenker M (2011) Noonan syndrome and clinically related disorders. Best Pract Res Clin Endocrinol Metab 25: 161-179.
8. de Ligt J, Willemsen MH, van Bon BW, Kleefstra T, Yntema HG, et al. (2012) Diagnostic exome sequencing in persons with severe intellectual disability. N Engl J Med 367: 1921-1929.
9. Bell JB, D.; Sistermans, E.; Ramsden, S.C. (2007) Practice guidelines for the Interpretation and Reporting of Unclassified Variants (UVs) in Clinical Molecular Genetics. Guidelines ratified by the UK Clinical Molecular Genetics Society (11th January, 2008) and the Dutch Society of Clinical Genetic Laboratory Specialists (Vereniging Klinisch Genetische Laboratoriumspecialisten; VKGL) (22nd October, 2007) http://www.cmgs.org/bpgs/pdfs%20current%20bpgs/UV%20GUIDELINES%20ratified.pdf.
10. Krieger E, Vriend G (2002) Models@Home: distributed computing in bioinformatics using a screensaver based approach. Bioinformatics 18: 315-318.
11. Venselaar H, Te Beek TA, Kuipers RK, Hekkelman ML, Vriend G (2010) Protein structure analysis of mutations causing inheritable diseases. An e-Science approach with life scientist friendly interfaces. BMC Bioinformatics 11: 548.
12. Jopling C, van Geemen D, den Hertog J (2007) Shp2 knockdown and Noonan/LEOPARD mutant Shp2-induced gastrulation defects. PLoS Genet 3: e225.
13. Software IJ http://rsb.info.nih.gov/ij/.
14. Thisse C, Thisse B (2008) High-resolution in situ hybridization to whole-mount zebrafish embryos. Nat Protoc 3: 59-69.
15. Yelon D, Horne SA, Stainier DY (1999) Restricted expression of cardiac myosin genes reveals regulated aspects of heart tube assembly in zebrafish. Dev Biol 214: 23-37.
16. Roach JC, Glusman G, Smit AF, Huff CD, Hubley R, et al. (2010) Analysis of genetic inheritance in a family quartet by whole-genome sequencing. Science 328: 636-639.
17. Marrero A, Duquerroy S, Trapani S, Goulas T, Guevara T, et al. (2012) The crystal structure of human alpha2-macroglobulin reveals a unique molecular cage. Angew Chem Int Ed Engl 51: 3340-3344.
18. Hong SK, Dawid IB (2008) Alpha2 macroglobulin-like is essential for liver development in zebrafish. PLoS One 3: e3736.
19. Runtuwene V, van Eekelen M, Overvoorde J, Rehmann H, Yntema HG, et al. (2011) Noonan syndrome gain-of-function mutations in NRAS cause zebrafish gastrulation defects. Dis Model Mech 4: 393-399.
20. Galliano MF, Toulza E, Gallinaro H, Jonca N, Ishida-Yamamoto A, et al. (2006) A novel protease inhibitor of the alpha2-macroglobulin family expressed in the human epidermis. J Biol Chem 281: 5780-5789.
21. Galliano MF, Toulza E, Jonca N, Gonias SL, Serre G, et al. (2008) Binding of alpha2ML1 to the low density lipoprotein receptor-related protein 1 (LRP1) reveals a new role for LRP1 in the human epidermis. PLoS One 3: e2729.
22. Geetha N, Mihaly J, Stockenhuber A, Blasi F, Uhrin P, et al. (2011) Signal integration and coincidence detection in the mitogen-activated protein kinase/extracellular signal-regulated kinase (ERK) cascade: concomitant activation of receptor tyrosine kinases and of LRP-1 leads to sustained ERK phosphorylation via down-regulation of dual specificity phosphatases (DUSP1 and -6). J Biol Chem 286: 25663-25674.
23. Takayama Y, May P, Anderson RG, Herz J (2005) Low density lipoprotein receptor-related protein 1 (LRP1) controls endocytosis and c-CBL-mediated ubiquitination of the platelet-derived growth factor receptor beta (PDGFR beta). J Biol Chem 280: 18504-18510.
24. Tartaglia M, Kalidas K, Shaw A, Song X, Musat DL, et al. (2002) PTPN11 mutations in Noonan syndrome: molecular spectrum, genotype-phenotype correlation, and phenotypic heterogeneity. Am J Hum Genet 70: 1555-1563.
25. Cordeddu V, Di Schiavi E, Pennacchio LA, Ma'ayan A, Sarkozy A, et al. (2009) Mutation of SHOC2 promotes aberrant protein N-myristoylation and causes Noonan-like syndrome with loose anagen hair. Nat Genet 41: 1022-1026.
26. Zenker M, Voss E, Reis A (2007) Mild variable Noonan syndrome in a family with a novel PTPN11 mutation. Eur J Med Genet 50: 43-47.
27. Variants DoG http://projects.tcag.ca/variation/.

Supplementary Information

Supplementary Clinical Descriptions of families with A2ML1 *mutations*

Family 1: c.2405G>A, p.(Arg802His), *de novo*

Case 1 This individual was referred because of hypotonia and facial dysmorphisms noticed directly after birth. Her parents were non-consanguineous, apparently healthy, and had no features suggestive for Noonan syndrome (NS). During pregnancy hygroma colli and polyhydramnion were noticed. Birth weight was 4005 gr. (+2 SD), length 49 cm (-0.5 SD). Clinical examination after birth showed short stature, developmental delay, typical Noonan syndrome facial features: a broad and high forehead, hypertelorism, low-set posteriorely rotated ears and webbed neck (Figure 1A). She had a broad thorax with widely spaced nipples (10,5 cm at 6 months of age) and pectus excavatum. Cardiologic evaluation revealed no structural heart defect. At 2 years the clinical diagnosis of NS was made. Her OFC at 12 years was 55 cm (+0,5 SD), at 15yrs and 9 months puberty stage : MIII,PIII-IV,A0. At16 years of age her height is 156 cm (-2 SD).
Of note, in this individual another *de novo* mutation was identified using exome sequencing being a missense change in *OR12D3* (NM_030959.2:c.386G>C). Evaluation of its pathogenicity in the context of the patients phenotype, however, excluded this variant as a likely cause.

Family 2: c.2405G>T, p.(Arg802Leu)

Case 2 The patient was referred together with his son. Clinical examination at the age of 48 years revealed general mild central hypotonia, height 181 cm (0 SD), weight 69,2 kg (0 SD), head circumference 58.1 cm (0SD). He had Noonan-like facial features with a high forehead, prominent eyes, slightly hypertelorism (intercanthal distance 3,6 cm at adult age , and thick hooded eyelids (Figure. 1B). Multiple pigmented nevi were noticed. The inter-nipple distance was 22cm at adult age. No heart abnormalities were seen. The patient was born prematurely at 34 weeks of gestation and stayed in an incubator for three months. He was part of a twin; His twin brother died at birth unexplained. He has social fears, performance anxiety and poor concentration.

Case 3 This individual is the son of case 2. He was born with a pulmonary valve stenosis. Physical examination at 11 years 9 months showed facial hypotonia with Noonan-like features (Figure 1B). His height was 155 cm (+0.5 SD), head circumference 54.5 cm (0SD), and intercanthal distance (2,9 cm) and genitalia were normal. The inter-nipple distance was 15,7 cm. Puberty was at Tannerstage 1-2 with no axillary hair. He walked clumsy with pes planus. His psychomotor development was mildly delayed. At the age of 6 years he was diagnosed with autistic-like behavior with attention deficit.

Case 4 This individual is the mother of case 2. She was healthy and had normal basic education. Examination at 73 years of age showed normal height and no facial dysmorphisms (Figure 1B). Cardiac evaluation revealed no abnormalities. No typical Noonan-like features were recognized.
Family 3: c.1775G>T, p.(Arg592Leu)

Case 5 This individual was referred in her second pregnancy. She has short stature with adult height of 157 cm (<-2 SD), facial features suggestive for Noonan syndrome and easy bruising (Figure 1C). The intercanthal distance was 3,4 cm at adult age. She had severe neonatal feeding problems, was clumsy and had an anxiety disorder at adult age. Her first menarche was at 12 years of age.

Case 6 This individual is the second child of case 5, and was born after 37 weeks of gestation with a birth weight of 3,195 gram and length of 50 cm. The intercanthal distance was 3,0 at 9 months (>+2SD). She had facial features suggestive for Noonan syndrome and bilateral hearing loss (30/40 dB) (Figure 1C). Cardiac evaluation revealed no abnormalities.

Case 7 This individual is the father of case 5. He has an adult height of 172 cm (-1,5 SD), relatively large head (OFC 59,5 cm (+ 1 SD)), hypertelorism (intercanthal distance 3,5 cm at adult age), a short broad neck. The inter-nipple distance was 25 cm at adult age. Cardiac evaluation revealed no abnormalities.

Case 8 This individual is the first child of case 5. The first pregnancy of case 5 ended at 29 weeks of gestation in an intra-uterine fetal death because of severe hydrops. There was polyhydramnios. The presence of MPS or a viral infection during pregnancy was excluded. Karyotyping and SNP array analysis on amniotic cells revealed no abnormalities. After birth, no pathologic examination has been done. The child had facial features compatible with Noonan syndrome. Analysis of fetal DNA material showed the same mutation as identified in his mother. There was insufficient amount of DNA left to exclude mutations in the other NS associated genes.

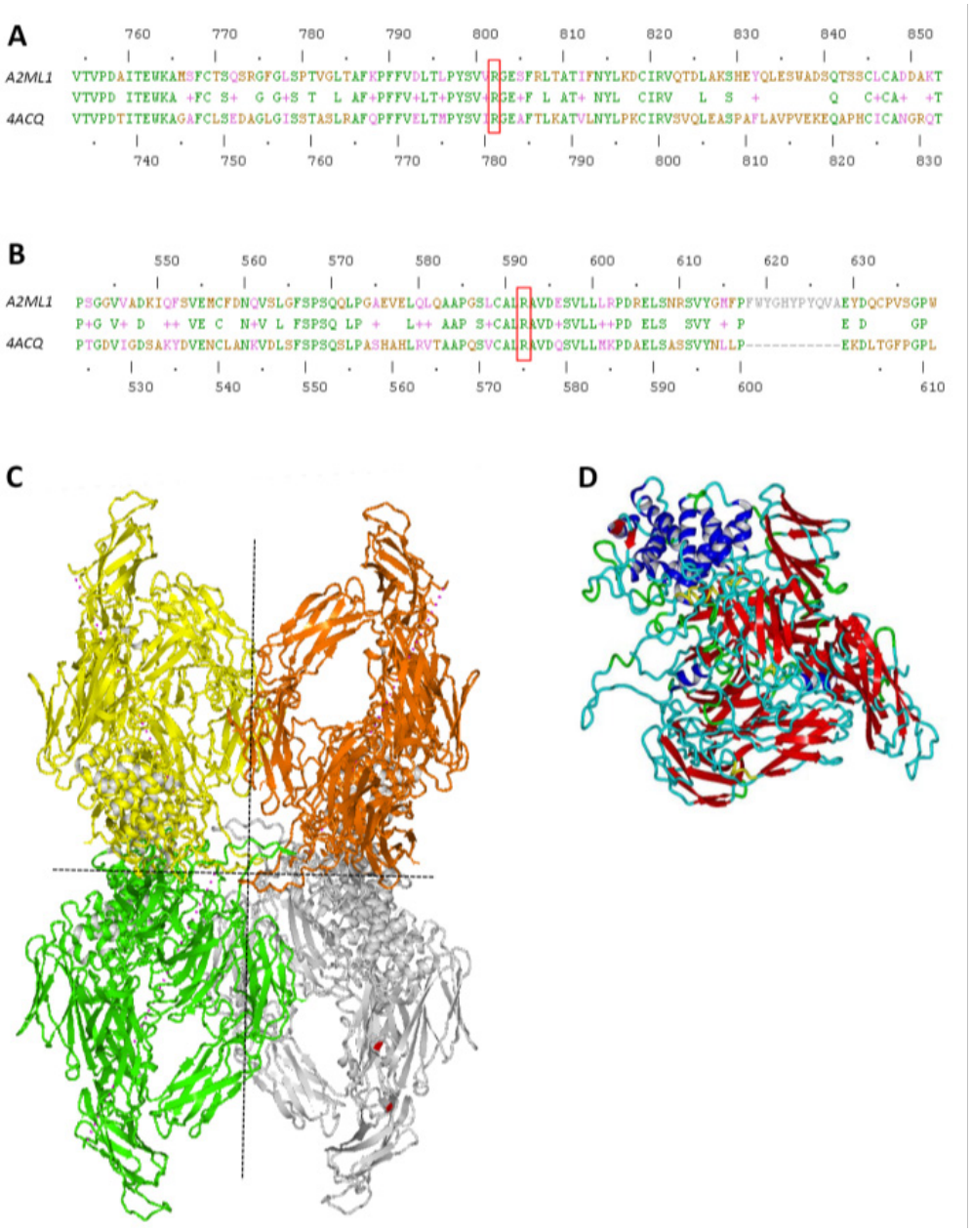

Supplementary Figure 1: Protein modeling of A2ML1 mutations
For protein modeling pdb file 4ACQ (representing A2M) was used, which shares 40% identity with A2ML1, and has positive scores for 57% and gaps for only 3% of sequence. Local protein alignments indicate that both affected amino acids are conserved in A2M (A,B, with the mutated residues highlighted in red boxes). A2ML1 proteins form a homotetrameric complex (C, with each monomer indicated by a different colour and dashed lines indicating planes of symmetry). The secondary structure of each of its monomers contains β-barrels (in red), that twist and coil to form a closed structure in which the beta-strands are arranged in an antiparallel fashion (D).

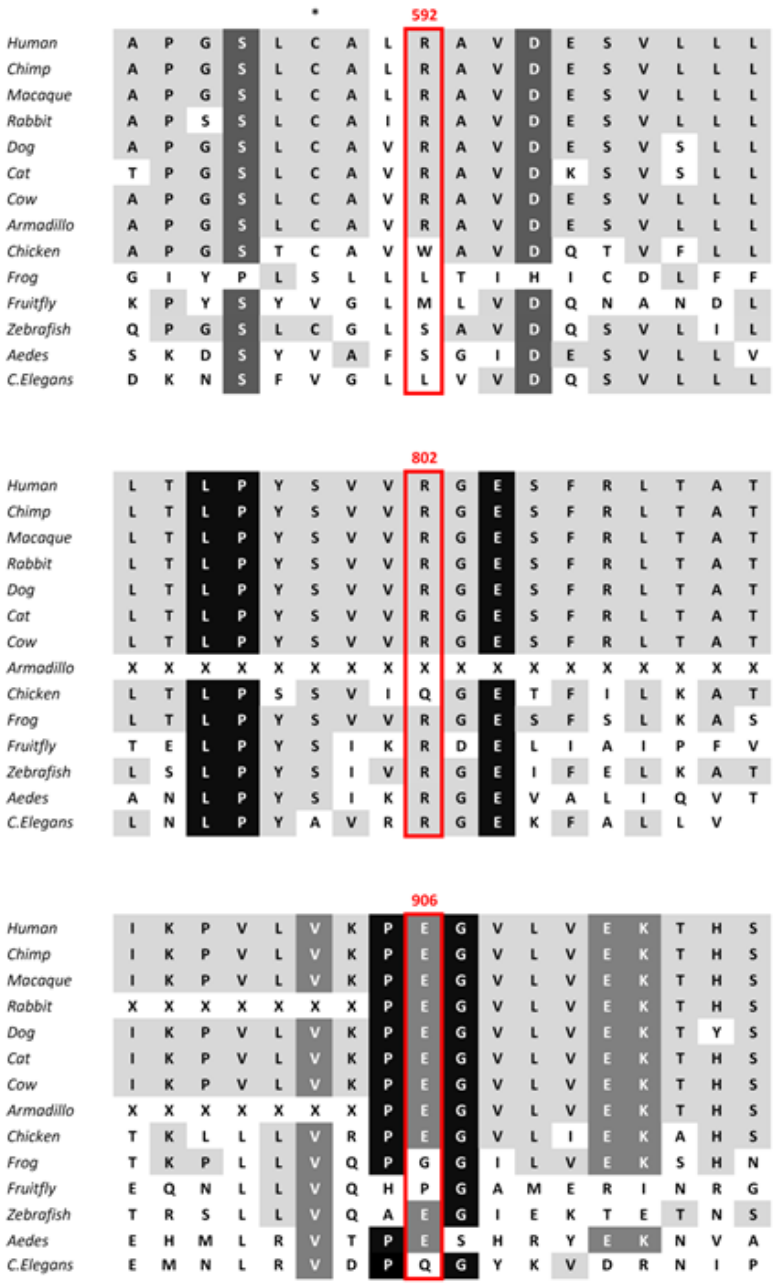

Supplementary Figure 2: Regional conservation of residues affected by mutations A2ML1 amino acid conservation across various species (listed on the left) for the residues affected by mutations. (A) Region surrounding p.Arg592 (highlighted in red box); note that p.Arg592 is not conserved in zebrafish A2ml1. (B) Region surrounding p.Arg802 (highlighted in red box), with full conservation in zebrafish. (C) Region surrounding p.Glu906, which is predicted to interact with p.Arg802 in wildtype A2ML1. This residue is conserved in Zebrafish. Asterisk in (A) represents cysteine involved in disulfide bridge formation.

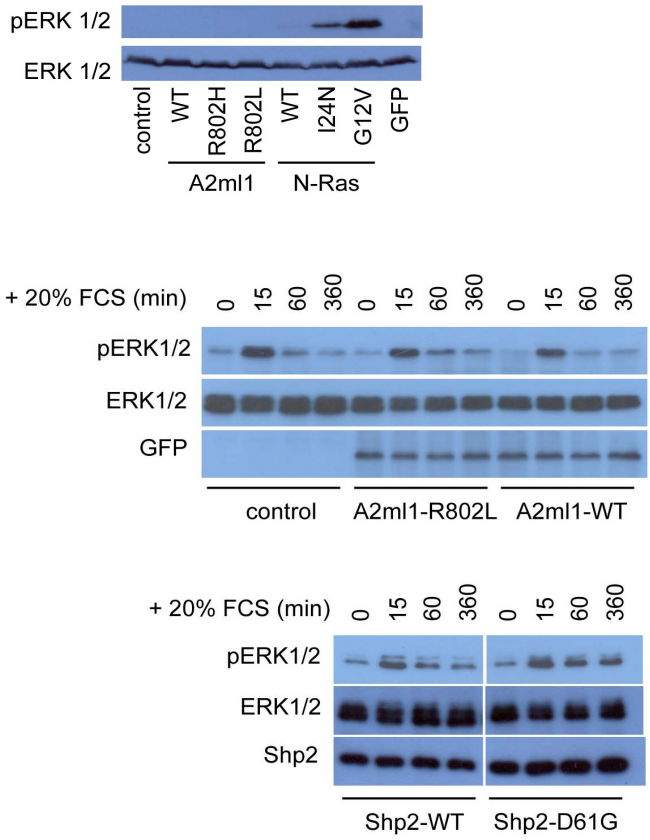

Supplementary Figure 3. Expression of mutant A2ml1 does not induce MAPK activation
(A) Human embryonic kidney HEK-293T cells were transfected with CMV-promoter-driven expression vectors for (mutant) A2ml1 or (mutant) N-Ras (known to induce MAPK activation). Cells were cultured in the presence of 10% fetal calf serum, lysed and the whole cell lysates were processed for immunoblotting using pERK1/2 specific antibodies and ERK1/2 specific antibodies to monitor protein levels. Expression of wild type (WT) and mutant A2ml1 (p.R802H or p.R802L) did not induce phosphorylation of ERK1/2, whereas NS-associated N-Ras-I24N induced mild activation and oncogenic N-Ras-G12V induced strong activation of ERK1/2. (B) Serum stimulation of COS7 cells expressing mutant A2ml1 did not affect ERK1/2 phosphorylation. COS7 cells were transfected with expression vectors encoding (mutant) A2ml1 or Shp2-D61G. Serum-starved cells were treated with 20% FCS for the indicated periods of time and subsequently, the cells were lysed and processed for immunoblotting using pERK1/2- and ERK1/2-specific antibodies. Expression of (mutant) A2ml1-GFP and (mutant) Shp2 was monitored using antibodies specific for GFP and Shp2, respectively. The ERK phosphorylation levels of wildtype (WT) and mutant A2ml1 expressing cells were indistinguishable, whereas ERK phosphorylation was enhanced in Shp2-D61G expressing cells. These results suggest either that A2ml1 does not modulate ERK/MAPK signaling, or that HEK-293T cells and COS7 cells are not responsive to A2ml1.

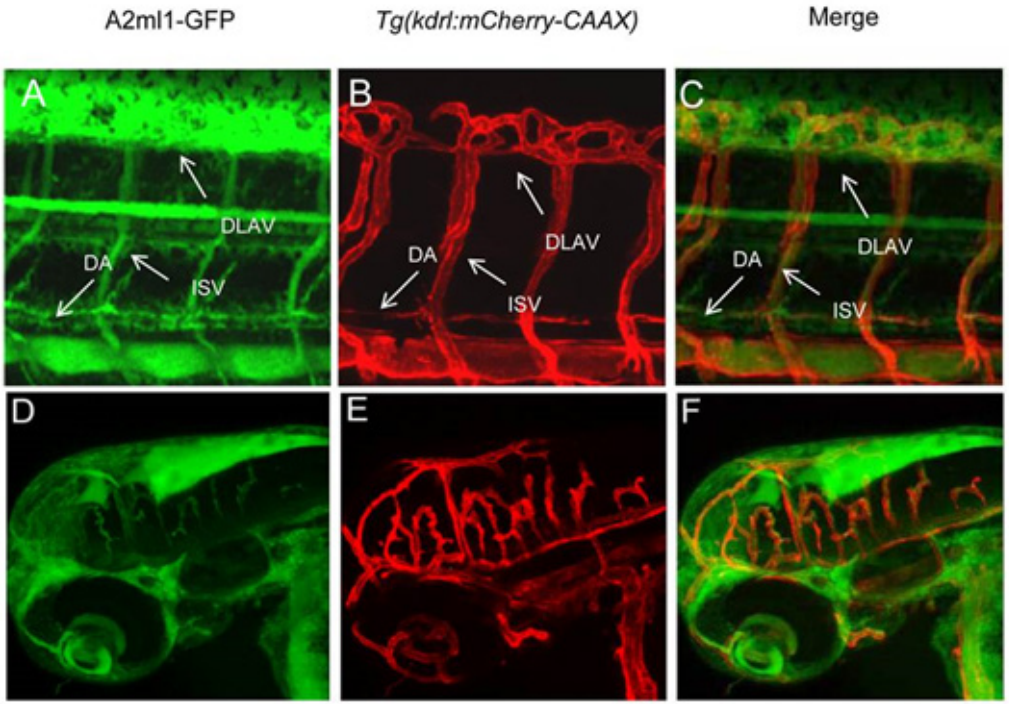

Supplementary Figure 4: A2ml1-GFP expression in zebrafish Expression of A2ml1-GFP was monitored in the transgenic reporter line Tg(kdrl:mcherry-CAAX) with expression of mCherry in all endothelial cells, thus highlighting vasculature. Zebrafish embryos were injected with plasmid DNA encoding a CMV-promoter-driven expression vector for A2ml1-GFP at the one-cell stage and imaged at 2 dpf. Lateral view of the trunk (A-C) and the head (D-F) are depicted. The dorsal aorta (DA), the Dorsal Longitudinal Anastomotic Vessel (DLAV) and intersegmental vessels (ISV) are indicated.

The expression patterns of A2ml1-GFP and mCherry were largely overlapping. A2ml1 is a secreted factor and these results confirm A2ml1-GFP localization throughout the vasculature system, even though not all cells express A2ml1-GFP due to mosaicism of the injected plasmid DNA.

Confocal imaging

Embryos at 48 hpf were dechorionated and mounted in glass-bottom 6-well plates using 0.25% agarose in E3 embryo medium containing 16 mg/ml 3-amino benzoic acid ethylester to block movements. Confocal imaging was performed using a SPE live confocal laser scanning microscope with 20x magnification for the head and 40x magnification for the trunk.

Raw sequencing statistics	**Case 1**	**Father**	**Mother**
Total number of mapped reads (Million)	56.02	79.73	59.88
Total number of bases mapped (Gb)	2.63	3.87	2.83
Total bases mapping to targets (Gb)	1.87	3.02	2.12
% mapping to target	71.10	78.04	74.91
% targets with 10x coverage	85.96	93.55	88.42
Mean target coverage	32.20	52.83	35.33
Median target coverage	39.14	66.87	45.28

Variant prioritization	**Case 1**
Total variants	23,021
*QC**	19,771
Located in coding sequence/canonical splice site	10,887
Leading to nonsynonymous change	5,063
*Excluding variants in controls***	124
Excluding variants inherited from healthy parent (possible de novo variants)	4

* ≥ 5 variant reads, ≥ 20% variantion reads
** dbSNPv130; in-house exome database

Supplementary Table 1: Raw sequencing statistics and variant prioritization

Exon	Variant (mRNA level)	Predicted protein effect	rs-number	Allele count over all populations (ESP)	Minor Allele Frequency 100%
*A. Presumable non-pathogenic variants**					
11	c.1123C>T	p.(=)	-	-	-
11	c.1215A>G	p.(=)	-	-	-
16	c.1918G>A	p.(Asp640Asn)	-	-	-
27	c.3287C>T	p.(Ser1096Phe)	-	-	-
B. Non-pathogenic variants					
2	c.105C>A	p.(=)	rs201185025	T=9/C=11923	0.08
2	c.186C>T	p.(=)	rs17792974	T=550/C=11532	4.55
3	c.289C>G	p.(Arg97Gly)	rs199701571	G=10/C=11922	0.08
5	c.463-9C>G	p.(?)	rs11047493	G=317/ C=11591	2.66
6	c.619G>C	p.(Gly207Arg)	rs11047499	C=329/G=12037	2.66
9	c.861C>A	p.(Asp287Glu)	rs61921916	A=124/C=12108	1.01
11	c.1101T>C	p.(=)	rs61744222	C=313/T=11763	2.59
11	c.1109T>C	p.(Phe370Ser)	rs61744220	C=310/T=11762	2.57
12	c.1275A>G	p.(=)	rs7308106	G=932/A=11214	7.67
12	c.1476+9G>A	p.(?)	rs7136813	A=3383/G=6475	34.32
15	c.1686T>G	p.(=)	rs12296765	G=102/T=9772	1.01
15	c.1777del**	p.(Ala593fs)	-	-	-
16	c.2026C>T	p.(Arg676Trp)	rs200503836	T=1/C=12065	0.09
18	c.2197T>C	p.(Phe733Leu)	rs117213221	C=3/T=11915	0.03
19	c.2367G>A	p.(=)	rs1860927	A=9912/G=2358	80.78
20	c.2550A>C	p.(Glu850Asp)	rs1860926	A=9644/C=372	96.29
22	c.2749T>C	p.(=)	rs200462659	C=7/T=12181	0.06
24	c.2868C>T	p.(=)	rs56179521	T=438/C=11740	27.24
24	c.2909G>A	p.(Cys970Tyr)	rs1558526	A=2356/G=10066	18.97
26	c.3237G>A	p.(=)	rs11612600	A=3769/G=8527	30.65
26	c.3252C>T	p.(=)	rs61745125	T=41/C=12247	0.33
27	c.3269G>A	p.(Gly1090Asp)	rs200964353	A=16/G=12812	0.12
27	c.3272T>C	p.(Val1091Ala)	rs61736726	C=172/T=12648	1.34
28	c.3364C>T	p.(Arg1122Trp)	rs1860967	T=3694/C=8552	30.16
29	c.3569C>T	p.(Ala1190Val)	rs73040625	T=742/C=11430	6.10
29	c.3676_3677del	p.(Ala1226fs)	rs144686314	-	2.1***
30	c.3686G>T	p.(Arg1229Leu)	rs10219561	G=11720/A=386	96.81
30	c.3769A>C/G	p.(Met1257Leu)	rs7308811	G=9457/A=2707	77.75
30	c.3843T>C	p.(=)	rs61749073	C=1326/T=10942	10.81
31	c.3878A>G	p.(Asn1293Ser)	rs201478459	G=10/A=12246	0.08
31	c.4020A>G	p.(=)	rs1476910	G=9125/A=3099	74.65
31	c.4061+1G>A****	p.(?)	rs202067416	A=6/G=10106	0.01

Supplementary Table 2: Presumable non-pathogenic variants detected by *A2ML1* sequencing (NM_144670.3)

*Parental DNAs not available for further segregation analysis. Guidelines for variant classification (see section Mutation interpretation) however predicts these variants to be non-pathogenic. As no rs-identifier is known for this variant, nor has been observed in 1000 genomes and/or ESP we cannot formally show its non-pathogenicity.
**Variant also detected in non-affected family members.
*** Minor Allele frequency from 1000 genomes project.
****For this variant segregation analysis was not possible. Since both c.1777del and c.3676_3677del are predicted to result in loss of function of the A2ML1 protein and are considered not pathogenic (see also under**), we hypothesize also the c.4061+1G>A is a rare non-pathogenic loss-of-function variant.